References

1. OH B., *The exponential law of endurance tests,* Am Soc Testing Mater Proc 1910. 10: p. 625–30.
2. Bannantine J.A., Comer J.J., and Handrock J.L., *Fundamentals of metal fatigue analysis*, Prentice Hall, Englewood Cliffs, New Jersey, 1989.
3. ASTM Standard: B108/B108M-08, 2009.
4. Heat Treatment, ASM Handbook, vol. 4, 1991.
5. Knez M., et al., *A rotating bending approach for determination of low-cycle fatigue parameters*, International Journal of Fatigue, 2010, 32 p. 1724-1730.
6. Stephens R.I., Fatemi, A., Fuchs H. O., John wiley & sons, *Metal fatigue in engineering*, canada, 2001.
7. Sachs, N. W., Understanding the surface features of fatigue fractures: How they describe the failure cause and the failure history. JFAPBC (2005), 2: 11-15
8. Haji Z.N., *Low cycle fatigue behavior of aluminum alloy AA2024-T6 and AA7020 T6.* Diyala Journal of Engineering Sciences, First Engineering Scientific Conference, college of engineering, university of diyala, 2010, p. 127-137.
9. Salerno G., Magnabosco R. and Neto C.d. M., *Mean strain influence in low cycle fatigue behavior of AA7175-T1 aluminum alloy*, International Journal of Fatigue, 2007, 29: p. 829-835.
10. Minichmayr R., Riedler M., Winter G., Leitner H. and Eichlreder W., *Thermo-mechanical fatigue life assessment of aluminium components using the damage rate model of Sehitoglu,* International Journal of Fatigue, 2008, 30: p. 298-304.

11. Neu RW, Sehitoglu H. Thermomechanical fatigue, oxidation and creep: part II. Life prediction, Metal Transction 1989, 20A:1755–81.
12. Prasad N. E., Gokhale A. A. and Rao P. R., *Mechanical behaviour of aluminium-lithium alloys,* in Sadhana (Academy Proceedings in Engineering Sciences), Indian Academy of Sciences, 2003, 28 (122) : P. 209-246.
13. Azadi M., *Effects of strain rate and mean strain on cyclic behavior of aluminum alloys under isothermal and thermo-mechanical fatigue loadings,* International Journal of Fatigue, 2013, 47: p. 148–153.
14. Mrowka-Nowotnik G.z. and Sieniawski J., *Influence of heat treatment on the microstructure and mechanical properties of 6005 and 6082 aluminium alloys,* Journal of Materials Processing Technology, 2005, p. 367–372.
15. Salazar-Guapuriche M., Zhao Y., Pitman A. and Greene A., *Correlation of Strength with Hardness and Electrical Conductivity for Aluminium Alloy 7010,* Materials Science Forum,Transction Technology Publications, Switzerland, 2006, 519-521: p. 853-858.
16. Marioara C.D., Anderson S. J., Jansen J. and Zardbergen H. W., *The influence of temperature and storage time at RT on nucleation of the β phase in a 6082 Al–Mg–Si alloy,* Acta Materialia , 2003, 51: p. 789–796.
17. Ortiz D., Abdelshahid M., Dalton R., Soltero J., Clark R., Han M., Lee E., Lightell W., Pregger B., Ogren J., Stoyanov P. and Es-Said O. S., *Effect of Cold Work on the Tensile Properties of 6061, 2024, and 7075 Al Alloys, JMEPEG,* ASM International, 2007, 16: p. 515-520, (DOI: 10.1007/s11665-007-9074-7 1059-9495).

18. Abdulwahab M., *Studies of the Mechanical Properties of Age-hardened Al-Si-Fe-Mn Alloy,* Australian Journal of Basic and Applied Sciences, 2008, 2(4): p. 839-843.
19. Siddiqui R.A., Abdul-Wahab S.A. and Pervez T., *Effect of aging time and aging temperature on fatigue and fracture behavior of 6063 aluminum alloy under seawater influence,* Materials and Design, 2008, 29: p. 70–79.
20. Al-Marahleh, G., *Effect of Heat Treatment on the Distribution and Volume Fraction of Mg2Si in Structural Aluminum Alloy 6063,* Metal Science and Heat Treatment, 2006, 48: p. 5-6.
21. Han S.-W., Katsumata K., Kumai S., Sato A., *Effects of solidification structure and aging condition on cyclic stress/strain response in Al/7% Si/0.4% Mg cast alloys,* Materials Science and Engineering, 2002, A337: p. 170-178.
22. Siddiqui R.A., Abdullah H.A. and Al-Belushi K.R., *Influence of aging parameters on the mechanical properties of 6063 aluminium alloy,* Journal of Materials Processing Technology, 2000, 102: p. 234-240.
23. Gupta A.K., Lloyd D.J. and Court S.A., *Precipitation hardening processes in an Al–0.4%Mg–1.3%Si–0.25%Fe aluminum alloy,* Materials Science and Engineering, 2001, A301: p. 140–146.
24. Gavgali M., Totik Y. and Sadeler R., *The effects of artificial aging on wear properties of AA 6063 alloy,* Materials Letters, 2003, 57: p. 3713– 3721.
25. Karamis M.B. and Halici I., *The effects of homogenization and recrystallization heat treatments on low-grade cold deformation properties of AA 6063 aluminum alloy,* Materials Letters, 2007, 61: p. 944–948.

26. Srivatsan T.S., *An investigation of the cyclic fatigue and fracture behavior of aluminum alloy 7055,* Materials and Design, 2002, 23: p. 141-151.
27. Borrego L.P., Abreu L.M., Costa J.M., Ferreira J.M., *Analysis of low cycle fatigue in AlMgSi aluminium alloys,* Engineering Failure Analysis, 2004, 11: p. 715–725.
28. Koh S.K., Oh S.J.,Li C., Ellyin F., *Low-cycle fatigue life of SiC-particulate-reinforced Al-Si cast alloy composites with tensile mean strain effects,* International Journal of Fatigue, 1999, 21: p. 1019-1032.
29. Hall J.N., Wayne Jones J. and A.K. Sachdev, *Particle size, volume fraction and matrix strength effects on fatigue behavior and particle fracture in 2124 aluminum-SiCp composites,* Materials Science and Engineering: A, 1994, 183: p. 69-80.
30. Ding H.-Z., Hartmann O., Biermann H., Mughrabi H., *Modelling low-cycle fatigue life of particulate-reinforced metal-matrix composites.* Materials Science and Engineering: A, 2002, 333: p. 295-305.
31. Chawla N., Jones J.W., Andres C., Allison J.E., *Effect of SiC volume fraction and particle size on the fatigue resistance of a 2080 Al/SiC p composite*, Metallurgical and Materials Transactions A, 1998, 29A: p. 2843-2854.
32. Hadianfard M.J. and Mai Y.-W., *Low cycle fatigue behaviour of particulate reinforced metal matrix composites,* Journal of Materials Sciences, 2006, 35: p. 1715 – 1723.
33. Shang J.K. and Ritchie R.O., *Crack Bridging by Uncracked Ligaments during Fatigue-Crack Growth in SiC-Reinforced Aluminum-Alloy Composites,* metallurgical transactions A, 1989, 20A: p. 897.

34. Muratoglu M., Yilmaz O. and Aksoy M., *Investigation on diffusion bonding characteristics of aluminum metal matrix composites (Al/SiCp) with pure aluminum for different heat treatments,* Journal of Materials Processing Technology, 2006, 178: p. 211–217.
35. Uygur I. and Kulekci M.K., *Low Cycle Fatigue Properties of 2124/SiCp Al-Alloy Composites,* Turkish Journal Engineering Enverment Science, 2002, 26: p. 265 - 274.
36. Li W., Chen Z.H., Chen D., Teng J., Fan C., *Low-cycle fatigue behavior of SiCp/Al–Si composites produced by spray deposition,* Materials Science and Engineering A, 2010, 527: p. 7631–7637.
37. Alan A. Luo, Robert C. Kubic, and John M. Tartaglia, *Microstructure and Fatigue Properties of Hydroformed Aluminum Alloys 6063 and 5754*, metallurgical and materials transactions, 2003, 34: p. 2549-2557.
38. Sha G., Keyna O., Brian C., John W., Richard H., *Growth related metastable phase selection in a 6xxx series wrought Al alloy,* Materials Science and Engineering A, 2001, 304–306 p. 612–616.
39. Tan E., *Influence of Heat Treatment on the Mechanical Properties of AA6066 Alloy,* Turkish Journal Engineering Enverment Science, 2007, p. 53 - 60.
40. Fatemi A.P., Khosrovaneh A.K., Tanner D., *Application of bi-linear log–log S–N model to strain-controlled fatigue data of aluminum alloys and its effect on life predictions,* International Journal of Fatigue, 2005, 27: p. 1040–1050.

41. Eleiche A.M., Megahed M.M. and Abd-Allah N.M., *Low-cycle fatigue in rotating cantilever under bending.III: Experimental investigations on notched specimens,* International Journal of Fatigue, 2006, 28: p. 271-280.
42. Manson S.S. and Dolan T., *Thermal stress and low cycle fatigue,* Journal of Applied Mechanics, 1966, 33: p. 957.
43. Megahed M.M., Eleiche A.M. and Abd-Allah N.M., *Low-cycle fatigue in rotating cantilever under bending I: Theoretical analysis,* International Journal of Fatigue, 1996, 18 (6): p. 401-412.
44. Zhang Z., Sun Q., Li C., and Zhao W., *Theoritical calculation of the strain hardening exponent and the strength coefficient of metallic materials,* Journal of material engineering performance,2006, 15: P. 19-22.
45. Smith K. N., Watson P. and Topper T. H., *A stress-strain function for the fatigue of metals*. J Mater JMLSA, 5(4): 767-778.
46. Chiou Y.C. and Yip M.C., *An energy-based damage parameter for the life prediction of AISI 304 stainless steel subjected to mean strain,* Journal of the Chinese institute of engineers, 2006, 29(3): p. 507-517.
47. Dowting N. E., *Mean stress effects in stress life and strain life fatigue*. SAE fatigue procedings of the third Intt. SAE fatigue congress.
48. Walker K., 1970, *The effect of stress ratio during crack propagation and fatigue for 2024-T3 and 7075-T6 aluminum , effects of enverement and couple load history on fatigue life,* ASTM STP, philadelphia (PA) , 462,P.1.
49. Barkanov E., *Introduction to the Finite Element Method,* Institute of Materials and Structures Faculty of Civil Engineering, Riga Technical University, Riga, 2001.

50. Szusta J. and Seweryn A., *Fatigue damage accumulation modelling in the range of complex low-cycle loadings-The strain approach and its experimental verification on the basis of EN AW-2007 aluminum alloy,* International Journal of Fatigue, 2011, 33: p. 255-264.
51. Saraev D. and Schmauder S., *Finite element modelling of Al/SiCp metal matrix composites with particles aligned in stripes-a 2D-3D comparison,* 2003, International Journal o Plasticity, 19: p. 733-747.
52. Aghdam M.M., Smith D.J., and Pavier M.J., *Finite element micromechanical modelling of yield and collapse behaviour of metal matrix composites,* Journal of the Mechanics and Physics of Solids, 2000, 48: p. 499-528.
53. Moraleda J.n., Javier S., and Javier L., *Finite deformation of incompressible fiber-reinforced elastomers: Acomputational micromechanics approach,* Journal of the Mechanics and Physics of Solids, 2009, 57: p. 1596–1613.
54. Boselli J., Pitcher P.D., Gregson P.J., Sinclair I., *Numerical modelling of particle distribution effects on fatigue in Al–SiCp composites,* Materials Science and Engineering, 2001, A300: p. 113–124.
55. ASTM Standard: B557M-10, 2010.
56. Fatigue and Fracture, ASM Handbook, vol. 19, 1996.
57. Chanrdupatla T. R., Belegundu A. D., *Introduction Finite Elements in Engineering*, second edition, prentice, Hall of India, private limited, New Delhi-110001, 1998.

58. Zuo, X. and Y. Jing, *Investigation of the age hardening behaviour of 6063 aluminium alloys refined with Ti, RE and B.* journal of materials processing technology 2009. 209: p. 360–366.
59. Kocanda, S., *Fatigue and Fracture* siijthoff & noordhoff international puplishers 1978. 1.

Appendix A

Procedure for calculating crystallite size

The sherrers' equation for crystallites size is given by

$$D = \frac{\text{Ks}\,\lambda}{\beta COS 2\theta_B} \qquad \text{(A.1)}$$

$\lambda = 1.54178 A^{\circ}$, $K_s = 0.9$ for instrumental (constant).

The diffraction of X-rays by crystals is explained in a very simple way by Bragg as being a specular reflection of parallel planes inside a crystal. Each set of planes have only certain angles, θ_B, and plane distances, d, that yield constructive interference, as seen in Fig. A.**1** Bragg's law for diffraction of X-rays with a wavelength, λ, from a crystal follows as:

$$2dsin\theta_B = n\lambda \qquad (A.2)$$

$$\beta^2 = \beta^2_{Total} - \beta^2_{Inst.} \qquad (A.3)$$

β^2_{Total} = 0.168: it is the value of FWHM (Full Width at Half Maximum intensity of the peak) from the experimental result at the Max. Intensity or Max. Peak for as received AA6063-T6 alloy as given in Table A.1.

$\beta^2_{Inst.}$ = 0.125 broudining of instrument

$$\beta^2 = \beta^2_{Total} - \beta^2_{Inst.} \qquad (A.4)$$

$= (0.168)^2 - (0.125)^2$

β^2 = 0.112245 deg

= 0.112245 $*\frac{\pi}{180}$

= 0.001959 (rad)

$\cos 2\theta_B = \cos 38.389 = 0.7838$ deg $= 0.7713$ Rad

$D = \frac{\text{Ks}\,\lambda}{\beta COS2\theta_B} = \frac{0.9\,(1.54178\,A^{\circ})}{(0.001959)(0.7713)}$ =918.34 A°

D = 91.834 nm

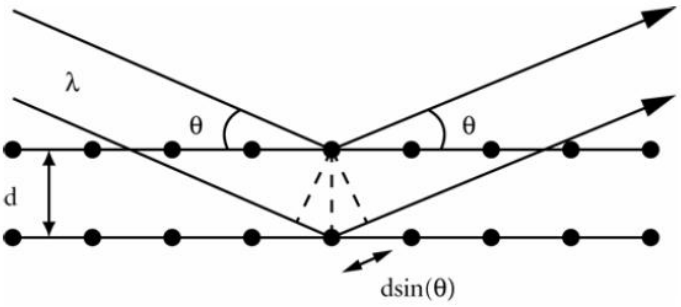

Fig. A.1 X-ray diffraction from two crystalline planes explaining Braggs law

Table A.1 X-RD experimental data for as-received AA6063-T6 alloy without loading

2-theta (deg)	ESD	d(ang.)	ESD	Height (cps)	ESD	FWHM (deg)	ESD	Int.I(cps deg)
38.3893	0.003667	2.34286	0.000215	3379.36	91.91519	0.1675	0.002826	716.41
44.6297	0.004554	2.02868	0.000196	2257.19	75.11977	0.1791	0.003826	509.44
64.9952	0.008725	1.43371	0.000171	426.14	32.63965	0.1965	0.010132	111.73
78.1121	0.006284	1.22251	8.26E-05	753.84	43.41187	0.2028	0.006489	211.58
82.3265	0.020014	1.17027	0.000234	163.31	20.20584	0.2152	0.01976	50.27

Tables A.2 to A.5 show experimental data for LCF tested samples at different load of as received AA6063samples.

Table A.2 X-RD experimental data for as-received AA6063-T6 alloy at 4.5 kg loading

2-theta(deg)	ESD	d(ang.)	ESD	Height(cps)	ESD	FWHM(deg)	ESD	Int.I(cps deg)
15.4025	0.119834	5.74802	0.044106	24.54	7.832031	1.6659	0.248019	50.75
38.3584	0.006286	2.34468	0.00037	1153.26	53.69504	0.1396	0.006783	219.9
44.6035	0.002217	2.02981	9.57E-05	7983.87	141.2787	0.1464	0.00235	1547.22
78.1075	0.008342	1.22257	0.00011	534.98	36.57124	0.1886	0.007803	145.36
82.3439	0.017985	1.17007	0.00021	132.65	18.21085	0.201	0.021345	41.34
98.9763	0.013807	1.01317	0.000104	400.33	31.63591	0.2817	0.014077	170.48

Table A.3 X-RD experimental data for as-received AA6063-T6 alloy at 6.9 kg loading

2-theta(deg)	ESD	d(ang.)	ESD	Height(cps)	ESD	FWHM(deg)	ESD	Int.I(cps deg)
15.219	0.331481	5.81693	0.123259	38.6	9.822884	2.8409	0.301394	116.71
28.5592	1.096282	3.12292	0.112998	3.42	2.924864	4.3573	1.158203	17.07
38.3689	0.015077	2.34405	0.000886	323.74	28.44929	0.1944	0.014543	86.65
40.0655	0.015588	2.24862	0.000839	137.19	18.51959	0.1227	0.021632	23.72
44.6327	0.001768	2.02855	7.62E-05	22692.39	238.1827	0.1386	0.001962	4218.03
78.1242	0.005092	1.22235	6.69E-05	1019.1	50.47516	0.1705	0.004543	246.22
98.9978	0.005234	1.013	3.95E-05	1794.44	66.97836	0.2042	0.006353	579.4

Table A.4 X-RD experimental data for as-received AA6063-T6 alloy at 7.389 kg loading

2-theta(deg)	ESD	d(ang.)	ESD	Height(cps)	ESD	FWHM(deg)	ESD	Int.I(cps deg)
14.2918	0	6.19213	0	1159.05	0	0.1552	0	272.2
38.3699	0.009575	2.344	0.000563	604.33	38.86921	0.1552	0.011554	136.48
44.6328	0.002582	2.02854	0.000111	8372.29	144.6746	0.1491	0.002779	1656.18
78.1335	0.00521	1.22223	6.85E-05	1621.6	63.67103	0.1593	0.004847	386.53
82.3451	0.007505	1.17006	8.76E-05	505.85	35.56163	0.1429	0.00648	99.19
98.9873	0.006005	1.01308	4.53E-05	1094.84	52.31733	0.1836	0.007869	325.19

Table A.5 X-RD experimental data for as-received AA6063-T6 alloy at 8.55 kg loading

2-theta(deg)	ESD	d(ang.)	ESD	Height(cps)	ESD	FWHM(deg)	ESD	Int.I(cps deg)
15.3357	0.345051	5.77293	0.126264	26.78	8.182451	2.2951	0.312594	65.43
38.3858	0.002708	2.34306	0.000159	12295.72	175.3262	0.1242	0.002643	1947.8
44.6088	0.002377	2.02958	0.000103	8094.41	142.2534	0.1405	0.002739	1548.89
78.1428	0.005202	1.22211	6.83E-05	1315.06	57.33798	0.1515	0.00495	292.95
82.3445	0.004323	1.17006	5.05E-05	1550.26	62.25476	0.1632	0.003721	357.58
98.9638	0.007432	1.01326	5.62E-05	510.47	35.72346	0.2005	0.011277	170.07

And calculated crystallite sizes (D) for their cases are AA6063/200 with 2 hours, AA6063/350 with 2 hours, AA6063/350 with 4 hours, AA6063/350 with 6 hours and AA6063/350 with 8 hours, respectively.

Similarly, Tables A.6 to A.10 show experimental data for AA6063/treated at 200℃ with soaking time 2 hours, AA6063/treated at 350℃ with soaking time 2 hours, AA6063/treated at 350℃ with soaking time 4 hours, AA6063/treated at 350℃ with soaking time 6 hours and AA6063/treated at 350℃ with soaking time 8 hours, respectively.

Table A.6 X-RD experimental data for AA6063-200℃ with soaked time 2hours

2-theta (deg)	ESD	d(ang.)	ESD	Height(cps)	ESD	FWHM (deg)	ESD	Int.I(cps deg)
38.6587	0.002173	2.32715	0.000126	6269.1	102.2179	0.1441	0.00188	1145.89
44.8985	0.002099	2.01715	8.94E-05	5079.19	92.00711	0.1506	0.002084	976.98
65.2422	0.005966	1.42888	0.000116	584.61	31.21457	0.1895	0.006524	139.78
78.3481	0.005089	1.21942	6.65E-05	931.72	39.40648	0.1954	0.004981	244.14
82.5653	0.007717	1.16749	8.95E-05	408.76	26.10099	0.1966	0.006928	105.73

Table A.7 X-RD experimental data for AA6063-350℃ with soaked time 2hours

2-theta(deg)	ESD	d(ang.)	ESD	Height(cps)	ESD	FWHM(deg)	ESD	Int.I(cps deg)
38.4753	0.002923	2.33782	0.000171	5436.3	134.6142	0.1412	0.002636	983.76
44.7117	0.00315	2.02515	0.000135	4971.37	128.7293	0.1566	0.003084	996.7
65.0187	0.019971	1.43325	0.000392	167.13	23.60314	0.2157	0.021697	45.92
78.1727	0.005511	1.22172	7.23E-05	1419.51	68.78726	0.2193	0.005748	405.69
82.3873	0.006857	1.16956	8.00E-05	830.84	52.62565	0.169	0.005544	184.31
99.0297	0.009972	1.01276	7.52E-05	483.61	40.15011	0.2436	0.008427	148.37

Table A.8 X-RD experimental data for AA6063-350℃ with soaked time 4hours

2-theta(deg)	ESD	d(ang.)	ESD	Height(cps)	ESD	FWHM(deg)	ESD	Int.I(cps deg)
38.4759	0.004839	2.33778	0.000283	3008.48	111.9612	0.1551	0.004071	601.45
44.6872	0.004677	2.0262	0.000201	3254.55	116.4502	0.2066	0.003392	819.35
65.0508	0.047696	1.43262	0.000934	102.25	20.64065	0.2848	0.040097	35.48
78.1579	0.009625	1.22191	0.000126	571.54	48.79992	0.24	0.010361	176.09
82.3614	0.018428	1.16987	0.000215	248.42	32.17273	0.2135	0.021488	70.76
98.9881	0.021567	1.01308	0.000163	190	28.13641	0.3093	0.02153	68.04

Table A.9 X-RD experimental data for AA6063-350C with soaked time 6hours

2-theta(deg)	ESD	d(ang.)	ESD	Height(cps)	ESD	FWHM(deg)	ESD	Int.I(cps deg)
38.3895	0.005127	2.34285	0.000301	3048.72	112.7075	0.1461	0.00467	575.02
44.6031	0.004312	2.02982	0.000186	3862.26	126.8572	0.1576	0.003861	763.35
64.9679	0.018857	1.43425	0.000371	153.11	25.25764	0.1702	0.021461	39.11
78.0905	0.005149	1.2228	6.77E-05	1521.99	79.63422	0.1593	0.004337	334.98
82.3054	0.009882	1.17052	0.000115	547.38	47.75731	0.1722	0.008271	126.73
98.8893	0.006635	1.01382	5.02E-05	514.12	46.28335	0.1984	0.010169	134.91

Table A.10 X-RD experimental data for AA6063-350 with soaked time 8hours

2-theta(deg)	ESD	d(ang.)	ESD	Height(cps)	ESD	FWHM(deg)	ESD	Int.I(cps deg)
15.2302	0.170626	5.81268	0.064017	27.13	10.63305	2.1891	0.449227	63.23
38.3626	0.009893	2.34443	0.000582	988.35	64.17266	0.1736	0.008968	238.01
44.6148	0.006112	2.02932	0.000264	1850.34	87.80517	0.1945	0.005306	461.16
64.9723	0.02077	1.43416	0.000408	103.55	20.77108	0.1821	0.02711	27.95
78.0986	0.010474	1.22269	0.000138	446.33	43.12438	0.239	0.011695	139.9
82.3433	0.047711	1.17008	0.000557	59.38	15.72891	0.2393	0.049786	19.94
98.9488	0.017829	1.01337	0.000135	183.01	27.61405	0.2492	0.01499	56.98

Also calculated crystallite sizes (D) for the cases AA6063/SiCp MMC with 2% V_f reinforcement particle and 2% V_f reinforcement particle .

Similarly, Tables A.11 and A.12 show experimental data for AA6063/SiCp MMC with 2% V_f reinforcement particle and 2% V_f reinforcement particle, respectively.

Table A.11 X-RD experimental data for AA6063/SiCp MMC with 2% V_f reinforcement particle

2-theta(deg)	ESD	d(ang.)	ESD	FWHM(deg)	ESD	Int.I(cps deg)
15.7085	0.443445	5.63673	0.153769	2.5357	0.411489	32.43
38.4309	0.010096	2.34042	0.000591	0.1705	0.007877	138.15
44.6841	0.007222	2.02633	0.000311	0.1639	0.007763	171.63
65.0324	0.010244	1.43298	0.000201	0.1943	0.01188	75.9
78.1379	0.00707	1.22217	9.29E-05	0.2099	0.007196	174.11
82.4199	0.023155	1.16918	0.00027	0.2102	0.024422	16.14
98.9592	0.026869	1.01329	0.000203	0.2308	0.025626	21.3
111.9128	0.023721	0.9296	0.00013	0.3124	0.021567	47.05
116.4478	0.038175	0.90609	0.000187	0.3623	0.032945	24.96

Table 12 X-RD experimental data for AA6063/SiCp MMC with 8% Vf reinforcement particle

2-theta(deg)	ESD	d(ang.)	ESD	FWHM(deg)	ESD	Int.I(cps deg)
38.3379	0.00532	2.34588	0.000313	0.1583	0.004291	312.86
44.5948	0.00625	2.03018	0.00027	0.1606	0.006745	199.99
64.9734	0.00534	1.43414	0.000105	0.17	0.005469	164.49
78.0757	0.007271	1.22299	9.57E-05	0.2118	0.007495	153.85
82.2956	0.017622	1.17063	0.000206	0.1944	0.018091	36.4
98.9337	0.036398	1.01349	0.000275	0.2524	0.046354	25.96
111.8877	0.015445	0.92974	8.47E-05	0.2423	0.020057	49.03
116.4375	0.016751	0.90614	8.21E-05	0.3288	0.02384	52.45